Artesunate induces G0/G1 cell cycle arrest and iron-mediated mitochondrial apoptosis in A431 human epidermoid carcinoma cells

Zhongyong Jiang[a,*], Jin Chai[b,*], Henry Hon Fung Chuang[d], Shifeng Li[c], Tianran Wang[a], Yi Cheng[a], Wensheng Chen[b] and Deshan Zhou[c]

The anticancer effects of artesunate (ART) have been well documented. However, its potential against skin cancer has not been explored yet. Herein we reported that 60 μmol/l ART effectively inhibited A431 (human epidermoid carcinoma cells) growth but not that of HaCaT (normal human keratinocyte cells). Our results revealed that ART induced cell cycle arrest at G0/G1 phase through the downregulation of cyclin A1, cyclin B, cyclin D1, Cdk2, Cdk4, and Cdk6. This correlated with the upregulation of p21 and p27. The 5-bromodeoxyuridine incorporation assay also indicated that ART treatment reduced DNA synthesis in a time-dependent manner. Furthermore, ART induced mitochondrial apoptosis, as evidenced by annexin V/propidium iodide staining and western blot analysis. Interestingly, ART-induced apoptosis diminished under iron-deficient conditions but intensified under iron-overload conditions. Taken together, these findings demonstrated the potential of ART in treating skin cancer through the induction of G0/G1 cell cycle arrest and iron-mediated mitochondrial apoptosis and supported further investigations in other test systems. *Anti-Cancer Drugs* **23:606–613** © **2012 Wolters Kluwer Health | Lippincott Williams & Wilkins.**

Anti-Cancer Drugs 2012, **23**:606–613

Keywords: A431 cells, apoptosis, artesunate, cell cycle, skin carcinoma

[a]Department of Clinical Laboratory, Chengdu Military General Hospital, Chengdu Military District, Chengdu, [b]Department of Gastroscopy, Southwest Hospital, Third Military Medical University, Chongqing, [c]Department of Histology and Embryology, School of Basic Medical Sciences, Capital Medical University, Beijing and [d]Department of Biochemistry and Cell Biology, Division of Life Science, Hong Kong University of Science and Technology, Hong Kong, China

Correspondence to Dr Deshan Zhou, Department of Histology and Embryology, School of Basic Medical Sciences, Capital Medical University, No.10 Xitoutiao, You An Men, Beijing 100069, China
Tel: +86 10 8391 1449; fax: +86 10 8391 1449;
e-mail: ds_zhou@126.com

*Zhongyong Jiang and Jin Chai contributed equally to the writing of this article.

Received 15 May 2011 **Revised form accepted** 31 December 2011

Introduction

Increased CO_2 emission, ozone depletion, and other environmental risk factors have led to a rising incidence of skin cancer in the past decades. It has been postulated that the free radicals generated by overexposure to sunlight primarily lead to DNA damage in skin cells and ultimately to skin cancers [1]. The nonmelanoma skin cancers, including basal cell carcinoma and squamous cell carcinoma, are the two most common forms of human skin malignant cancer, with over a million new cases each year worldwide [2]. Although skin cancer can often be treated with surgery, chemotherapy, or radiation therapy, the risk of recurrence and metastasis remains a concern [2]. Hence, continuous efforts have been made to pursue and develop additional approaches to treating skin cancer more effectively.

Artemisinin, a natural sesquiterpene extracted from a Chinese plant abrotani herba, is a traditional antimalarial drug that possesses anticancer potential [3–5]. Its water-soluble derivative, artesunate (ART), also exhibited comprehensive cytotoxicity toward a wide range of cancer cell lines including leukemia, melanomas, breast, ovarian, prostate, and renal cancer cells [4,6]. In-vivo experiments also demonstrated its anticancer effects in pancreatic cancer, cervical cancer, lung cancer, and colorectal cancer [7–10]. Nevertheless, the molecular mechanism underlying the anticancer potential of ART has been poorly studied. It has been speculated that ART induces apoptosis and disrupts cell cycle regulation [9,11]. Recent findings also implicated the pivotal role of the intracellular iron level in ART-induced apoptosis [12–17]. Structurally, ART enclosed an endoperoxide bridge that acted in response with ferrous iron to generate reactive oxygen species in cancer cells, leading to cancer cell death [12–14].

Although the anticancer effects of ART have been well documented for decades, its potential against skin cancer has not yet been explored. Therefore, the present study aimed to evaluate the potential anticancer effects of ART in skin cancer and demonstrated its inhibitory mode of action in A431 (human epidermoid carcinoma cells) through G0/G1-phase cell cycle arrest and iron-mediated mitochondrial apoptosis. These findings will provide the basis for further investigation in other test systems.

Materials and methods

Compounds and antibodies

Reagents 3-(4,5-dimethylthiazol-yl)-2,5-diphenyltetrazoliumbromide (MTT), 5-bromodeoxyuridine (BrdU), 4′,6-diamidino-2-phenylindole (DAPI), dimethyl sulfoxide, ribonuclease A, deferoxamine mesylate (DFOM), and

0959-4973 © 2012 Wolters Kluwer Health | Lippincott Williams & Wilkins DOI: 10.1097/CAD.0b013e328350e8ac

$FeSO_4$ were purchased from Sigma–Aldrich (St Louis, Missouri, USA). ART was purchased from Nan Fang pharmaceutical factory (Guilin, China). Dulbecco's modified Eagle's medium (DMEM), penicillin–streptomycin, and fetal bovine serum (FBS) were purchased from Gibco BRL (San Diego, California, USA). The annexin V-FITC kit was purchased from BD Pharmingen (San Diego, California, USA). The primary antibodies for Bax, Bcl-2, caspase-3, survivin, Cdk2, Cdk4, Cdk6, cyclin A1, cyclin D1, cyclin B, p21, p27, BrdU, and GAPDH were purchased from Santa Cruz Biotechnology (Santa Cruz, California, USA). Horseradish peroxidase-labeled IgG and Cy3-conjugated IgG were purchased from DAKO (Carpinteria, California, USA).

Cell culture

A431 cells (human epidermoid carcinoma cells) and HepG2 (human hepatocellular carcinoma cells) were obtained from the American Type Culture Collection (Manassas, Virginia, USA). The HaCaT cell line (spontaneously immortalized human keratinocytes cells) was obtained from the German Cancer Research Center (Heidelberg, Germany). The cells were maintained in DMEM medium containing 100 units/ml penicillin and 100 μg/ml streptomycin with 10% heat-inactivated FBS in a humidified atmosphere of 95% air and 5% CO_2 at 37°C.

Cell proliferation assay

A431 cells were seeded at a density of 5×10^3 cells/well in 96-well plates (Corning Glass Works, Corning, New York, USA) and incubated with 1% FBS for 12 h to synchronize cells in G0 phase and then treated with or without ART at indicated concentrations for 24 or 48 h, respectively. To generate iron depletion or overload condition, the cells were pretreated with 60 μmol/l DFOM or 60 μmol/l $FeSO_4$ for 4 h before ART treatment. Cell viability was measured by the MTT assay. Briefly, the cells were incubated with MTT solution (5 mg/ml) at 37°C for 4 h. Then, the medium was removed and crystals were dissolved in 100 μl dimethyl sulfoxide. Absorbance was measured at a wavelength of 570 nm using a Model 680 microplate reader (Bio-Rad, Hercules, California, USA). All the experiments were repeated at least three times.

Quantitative analysis of apoptotic cells by annexin V/propidium iodide staining

A431 and HaCaT cells were plated at a density of 1×10^5 cells in 60-mm dishes to synchronize cells at G0 phase and treated with ART as described earlier. After treatment, cells were collected for double staining with FITC-conjugated annexin V and propidium iodide (PI) according to the manufacturer's instructions. The stained cells were subsequently analyzed using flow cytometry. Generally, living cells were indicated by being double negative for annexin V and PI. Early apoptotic cells were indicated by being annexin V positive and PI negative (Q4), and late apoptotic and necrotic cells were indicated by being annexin V and PI double positive (Q2). All the experiments were repeated at least three times.

Cell cycle analysis using flow cytometry

After being synchronized, A431 cells were incubated with 60 μmol/l ART for 24 or 48 h. Thereafter, cells were harvested and fixed in 75% ethanol at 4°C overnight. After washing with PBS three times, the cells were labeled with 10 μg/ml PI containing 100 U/ml DNase-free ribonuclease A at 25°C in the dark for 30 min. DNA contents were determined by counting the incorporation of PI into DNA using flow cytometric analysis.

5-Bromodeoxyuridine incorporation assay

A431 cells were grown on coverslips in DMEM with 1% FBS for 12 h and then treated with 60 μmol/l ART for 24 or 48 h. BrdU (10 μmol/l) was added to the culture medium for 2 h after treatment. The coverslips were fixed in 4% paraformaldehyde for 12 h at 4°C. After rinsing in PBS, the cells were treated with 2 N HCl for 20 min at 37°C. Then, the specimens were incubated with a mouse monoclonal antibody raised against BrdU (3 μg/ml) at 4°C overnight and then revealed using a Cy3-conjugated secondary anti-mouse IgG with 1/100 dilution for 30 min at room temperature (RT). The nuclei of cells were visualized using DAPI with 1/5000 dilution. Finally, the coverslips were washed again and mounted for observation on a BX51 fluorescence microscope (Olympus, Tokyo, Japan).

Caspase-3 activity assay

The caspase-3 activity assay was performed using a CaspGLOW Fluorescein-Active Caspase-3 Staining Kit (Biovison, Mountain View, California, USA) according to the manufacturer's instructions. Briefly, A431 cells were treated with ART for 0, 4, 8, 12, and 24 h. Thereafter, cells were collected and stained with FITC–DEVD–FMK for 1 h in an incubator at 37°C with 5% CO_2. After rinsing twice with wash buffer, the cells were subjected to flow cytometric analysis using the FL-1 channel.

Western blot analysis

The cells were synchronized and incubated with ART as described above. Whole cell extracts were prepared in lysis buffer containing 50 mmol/l Tris-Cl, 150 mmol/l NaCl, 0.5% Nonidet P-40, 50 mmol/l NaF, 1 mmol/l Na_3VO_4, 5 mmol/l glycerophosphate, 1 mmol/l phenylmethylsulfonyl fluoride, 1 mmol/l dithiothreitol, pH 7.5, and centrifuged at 12 000 g for 20 min. The proteins were stored at −80°C until use, and protein concentration was determined by the bicinchoninic acid method. For western blot, an equal amount of protein for each sample was loaded onto 10 or 12% SDS-PAGE gels. After electrophoresis, the proteins were transferred to a polyvinylidene fluoride membrane and blocked in Tris-buffered saline containing 0.05% Tween-20 (TBS-T) with 5% nonfat dried milk for 1 h at RT. All primary antibodies with

1/1000 dilution were incubated for 2 h at RT or at 4°C overnight, and then membranes were washed three times in TBS-T before labeling with the secondary peroxidase-conjugated goat anti-rabbit/mouse IgG antibody (1 : 2000). The immunoblots were visualized with enhanced chemiluminescence substrate solution (Amersham Pharmacia Biotech, Piscataway, New Jersey, USA) according to the manufacturer's instructions, followed by exposure to radiographic film. GAPDH was used as an internal control. Blots shown are representative of three independent experiments.

Statistical analysis

All data are expressed as means ± SEM from at least three independent experiments. Statistical analyses were carried out with the unpaired Student *t*-test. Group differences at the level of P less than 0.05 were considered statistically significant.

Results

Artesunate treatment effectively inhibits A431 cell growth

The growth inhibitory effect of ART on A431, HepG2, and HaCaT cells was examined at various concentrations ranging from 30 to 210 μmol/l for 48 h using MTT assay. As shown in Fig. 1, ART significantly inhibited the growth of A431 cells in a concentration-dependent manner commencing at 60 μmol/l. However, at this concentration, HaCaT cells showed resistance toward ART. The estimated IC_{50} value of ART on A431, HepG2, and HaCaT cells was 60, 50, and 120 μmol/l, respectively. Thus, to maintain the growth inhibitory effect of ART in A431 cells without causing major side effects in HaCaT cells, 60 μmol/l of ART was used in subsequent experiments.

Artesunate treatment induces G0/G1-phase cell cycle arrest

Given the evidence of growth inhibition on A431 cells under ART treatment, the cell cycle distribution was examined using flow cytometry. Flow cytometric analysis showed that ART treatment increased the cell numbers at G0/G1 phase with decreased cell numbers at S-phase in a time-dependent manner. Of the cell population, 56.8 and 70.77% were arrested at the G1 phase after 24 and 48 h of ART treatment, respectively (Fig. 2a). Only 18.87 and 4.42% of the ART-treated cells underwent the S-phase after 24 and 48 h (Fig. 2a). A continuous reduction of BrdU incorporation was also observed in ART-treated cells (Fig. 2b). Consistent with flow cytometric analysis, ART upregulated the expression of cyclin A1, cyclin B, cyclin D1, Cdk2, Cdk4, and Cdk6 and downregulated cyclin inhibitors p21 and p27 (Fig. 2c).

Artesunate treatment induces apoptosis

The growth inhibitory effect of ART may be associated with the induction of apoptosis [18,19]. To quantify

Fig. 1

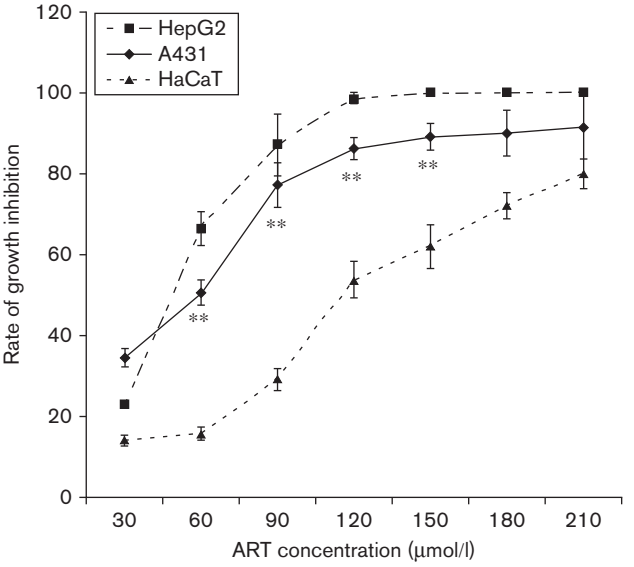

Effects of artesunate (ART) on the rate of cell growth inhibition. A431, HepG2, and HaCaT cells were incubated with 30–210 μmol/l ART for 48 h. Cell viability was analyzed using the MTT assay. The rate of growth inhibition was calculated as: inhibition rate of growth inhibition $=(1-OD570_{treat}/OD570_{con})\times 100\%$, where $OD570_{treat}$ is OD570 of the ART-treated group and $OD570_{con}$ is OD570 of the control group. $^{**}P<0.01$, compared with HaCaT cells. Data shown are means ± SEM of three independent experiments carried out in triplicate. OD, optical density.

ART-induced apoptosis, A431 and HaCaT cells were stained with annexin V and PI after 48 h of ART treatment and analyzed using flow cytometry. ART significantly increased the number of both early apoptotic cells (Q4, annexin V positive, PI negative) and late apoptotic or necrotic cells (Q2, annexin V positive, PI positive) of A431, whereas no significant apoptotic effect of ART was found on HaCaT cells (Fig. 3a and b).

Artesunate-induced cell cycle arrest occurs before apoptosis

Cell cycle arrest is often accompanied by apoptosis. To address whether ART-induced cell cycle arrest occurred before the onset of cell apoptosis, a time-course observation on cell cycle and apoptosis was made using flow cytometric analysis and the caspase-3 activity assay, respectively. Interestingly, we found that 8 h of ART treatment was able to induce cell cycle arrest at G0/G1 phase (Fig. 4a), whereas no significant apoptotic cells were observed at this time point, as presented by low caspase-3 activation (Fig. 4b) and few annexin V-positive cells (Fig. 4c). Apoptotic cells were only detected after 12 h of ART treatment, suggesting that disruption of cell cycle occurred before apoptosis in A431 cells upon ART treatment.

Fig. 2

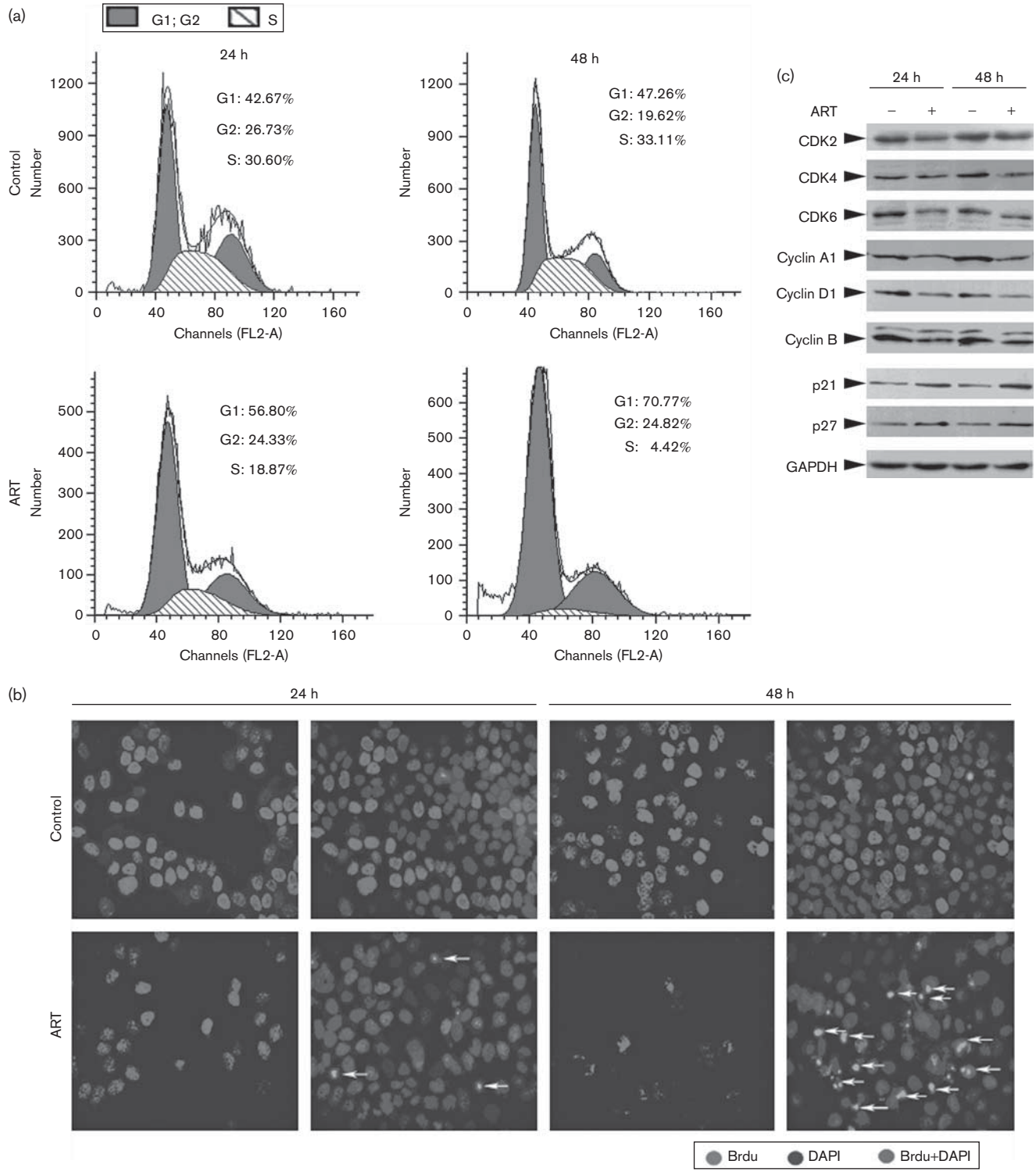

Cell cycle analysis of A431 cells treated with 60 μmol/l artesunate (ART). (a) A431 cells were treated with 60 μmol/l ART for 24 and 48 h and stained with propidium iodide. Flow cytometry was used to analyze DNA content at the G0/G1, S, and G2/M phases of the cell cycle. Data are representative of three similar experiments. (b) 5-Bromodeoxyuridine (BrdU) incorporation was performed to analyze the rate of DNA synthesis in A431 after ART treatment (in panel 1 and 3). Cell nuclei were then visualized by DAPI staining (in panel 2 and 4). Arrows indicate apoptotic features (nuclear condensation and nuclear fragmentation). (c) After treatment of A431 cells with 60 μmol/l ART for 24 and 48 h, the expression of cell cycle protein including cyclin A1, cyclin B1, cyclin D1, Cdk2, Cdk4, Cdk6, p21, and p27 were analyzed by western blots. Data are representative of three independent experiments.

Fig. 3

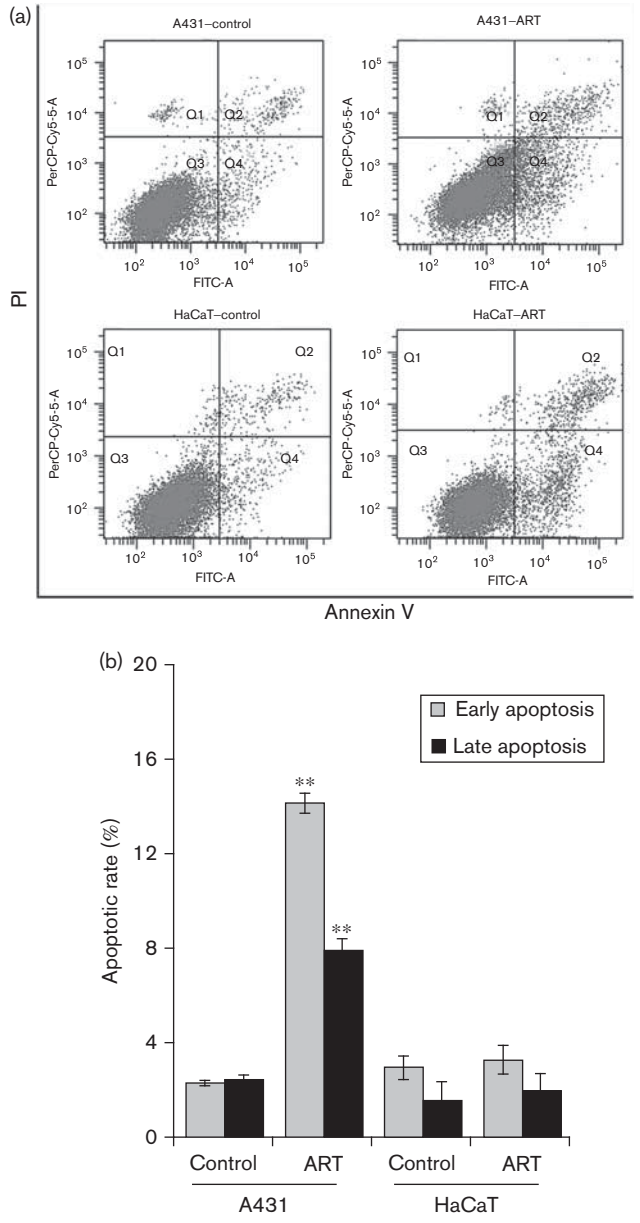

Flow cytometric analysis of artesunate (ART)-induced apoptosis using FITC-annexin V/propidium iodide (PI) staining. (a) A431 and HaCaT cells were treated with 60 μmol/l ART for 48 h and stained with FITC-annexin V/PI. Apoptotic and necrotic cell populations were analyzed using flow cytometry. Cells in the lower right quadrant (Q4) represent early apoptotic cells and cells in the upper right quadrant (Q2) represent late apoptotic and necrotic cells. Data are representative of three similar experiments. (b) Quantitative analysis of apoptotic cells after ART treatment. $^{**}P<0.01$, compared with vehicle control. Data shown are means ± SEM of three independent experiments.

Cellular iron level mediates artesunate-induced apoptosis

Previous studies have implicated the pivotal role of intracellular iron level in ART-induced apoptosis in cancer cells [18,19]. Therefore, we examined ART-induced apoptosis in A431 cells under iron-deficient (DFOM) or overload ($FeSO_4$) condition. As shown in Fig. 5, the ART-induced apoptotic cells significantly decreased in cells pretreated with DFOM for 4 h but increased significantly in cells pretreated with $FeSO_4$ for 4 h. DAPI staining further confirmed this finding, showing less nucleus shrinkage and condensation in ART + DFOM-treated cells and more so in ART + $FeSO_4$-treated cells (Fig. 5c). Remarkably, the iron-deficient condition induced by DFOM antagonized the upregulation of Bax and caspase-3 and downregulation of Bcl-2 and survivin by ART, whereas the iron-overload condition induced by $FeSO_4$ enhanced the upregulation of Bax and caspase-3 and downregulation of Bcl-2 and survivin by ART (Fig. 5d).

Discussion

The present study serves as the starting point for future investigation of ART against skin cancer. To our knowledge, we are the first to demonstrate the anticancer potential of ART in A431 cells. ART selectively inhibited A431 cell growth commencing at 60 μmol/l after 48 h. The IC_{50} of ART on A431 cells (~60 μmol/l) is nearly half of that in HaCaT (~120 μmol/l), indicating the specificity of ART in skin cancer cells and hence its potential as a novel anti-skin cancer drug with few side effects.

Overall, our results showed that the anticancer effect of ART in A431 cells was contributed by two mechanisms: (a) cell cycle arrest and (b) apoptosis. A previous study has reported G2/M cell cycle arrest in prostate cancer cells upon ART treatment [7,20,21]. In the present work, we also found an induction of cell cycle arrest, although at G0/G1 phase. Upon 24 and 48 h of ART treatment, the cell number proportionally increased at G0/G1 phase and decreased at S phase. Indeed, a striking reduction of BrdU incorporation in ART-treated cells in a time-dependent manner indicates a reduced rate of DNA synthesis after ART treatment. We also found that several cell cycle regulatory protein expressions responsible for G0/G1-phase progression, such as cyclin A1, cyclin D1, Cdk2, Cdk4, and Cdk6, were downregulated by ART. Correspondingly, Cdk inhibitory protein, p21, and p27 were upregulated by ART.

It has been documented that ART induces caspase-3-dependent apoptosis in various cancer cell lines [5]. Annexin V/PI staining supported this finding, showing increased number of early apoptotic cells (Q4, annexin V positive, PI negative) and late apoptotic or necrotic cells (Q2, annexin V positive, PI positive) upon ART treatment in A431 cells. Typical apoptotic morphologies and upregulation of proapoptotic proteins (Bax and caspase-3) as well as downregulation of antiapoptotic proteins (Bcl-2 and survivin) were observed in the present work, suggesting that ART possibly induced apoptosis in A431 cells through the mitochondrial intrinsic pathway [18,19].

It has been reported that ART enclosed an endoperoxide bridge that cleaved in response to ferrous iron to form

Fig. 4

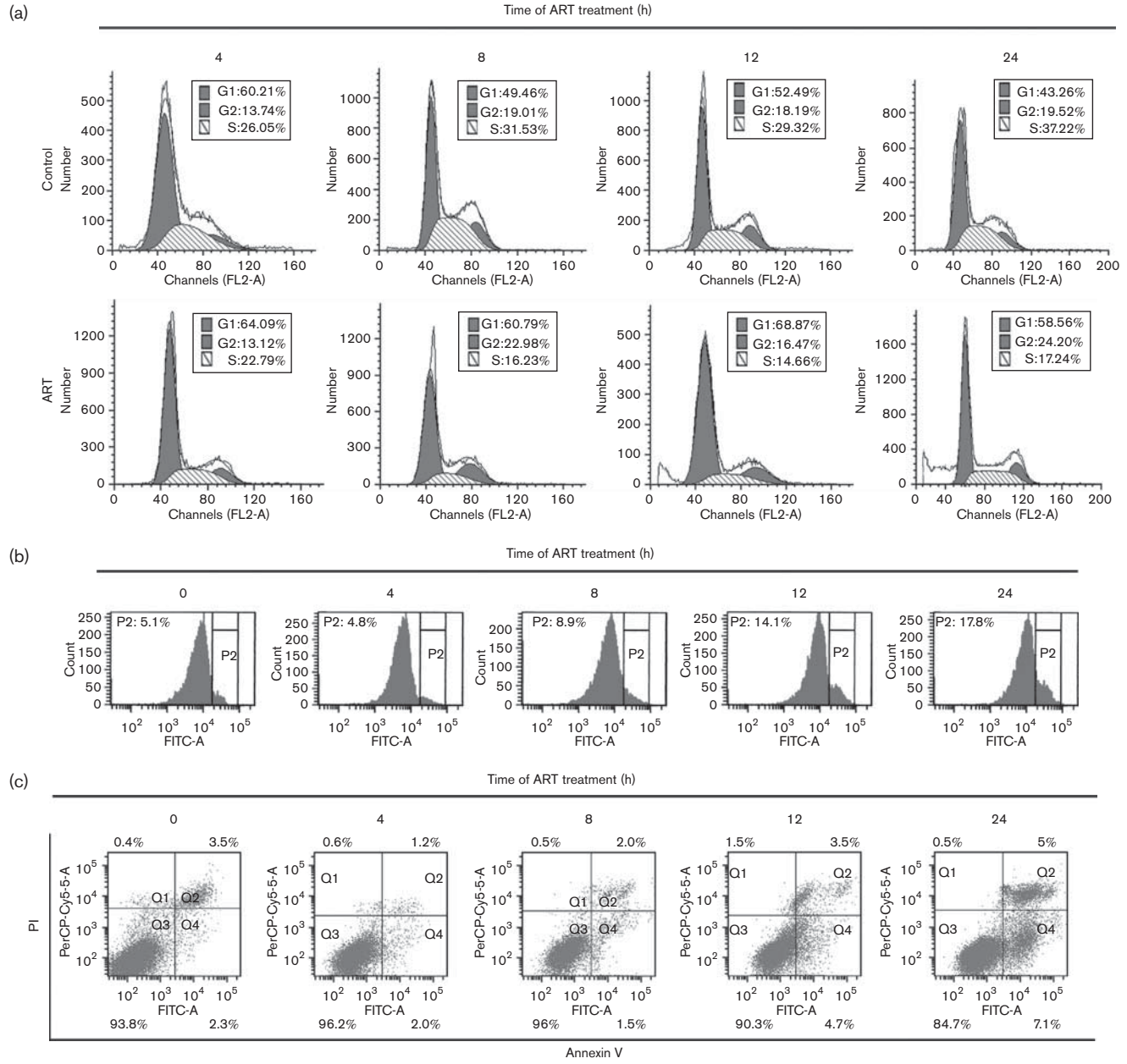

Time-course observation of artesunate (ART)-induced cell cycle arrest and apoptosis by flow cytometric analysis and caspase-3 activity assay. A431 was treated with 60 μmol/l ART for 0, 4, 8, 12, and 24 h as indicated. Thereafter, cells were subjected to cell cycle analysis by (a) flow cytometric assay, (b) caspase-3 activity assay, and (c) apoptosis analysis by FITC-annexin V/propidium iodide (PI) staining, respectively. P2 region in (b) indicated for the number of cells with caspase-3 activation.

free radicals within mitochondria and ultimately killed the cancer cells by excessive oxidative stress and apoptosis [10,22–24]. Indeed, we found that iron mediated the ART-induced apoptosis in A431 cells. In the presence of the iron chelator desferoxamine (DFOM), ART-induced apoptotic cells were significantly decreased with less nucleus shrinkage and chromatin condensation. The down-regulation of antiapoptotic protein (Bcl-2 and survivin) and upregulation of proapoptotic protein (Bax and caspase-3) were also inhibited. Therefore, we speculated that ART exerted its anticancer effects in A431 cells in part by first generating iron-dependent oxidative stress and then triggering the mitochondrial apoptosis. However, the exact mechanism by which cellular iron level regulated ART-induced apoptosis in A431 cells has yet to be determined. It would be of interest to simultaneously examine other oxidative stress response proteins, including catalase and glutathione *S*-transferase, both of which affected the

Fig. 5

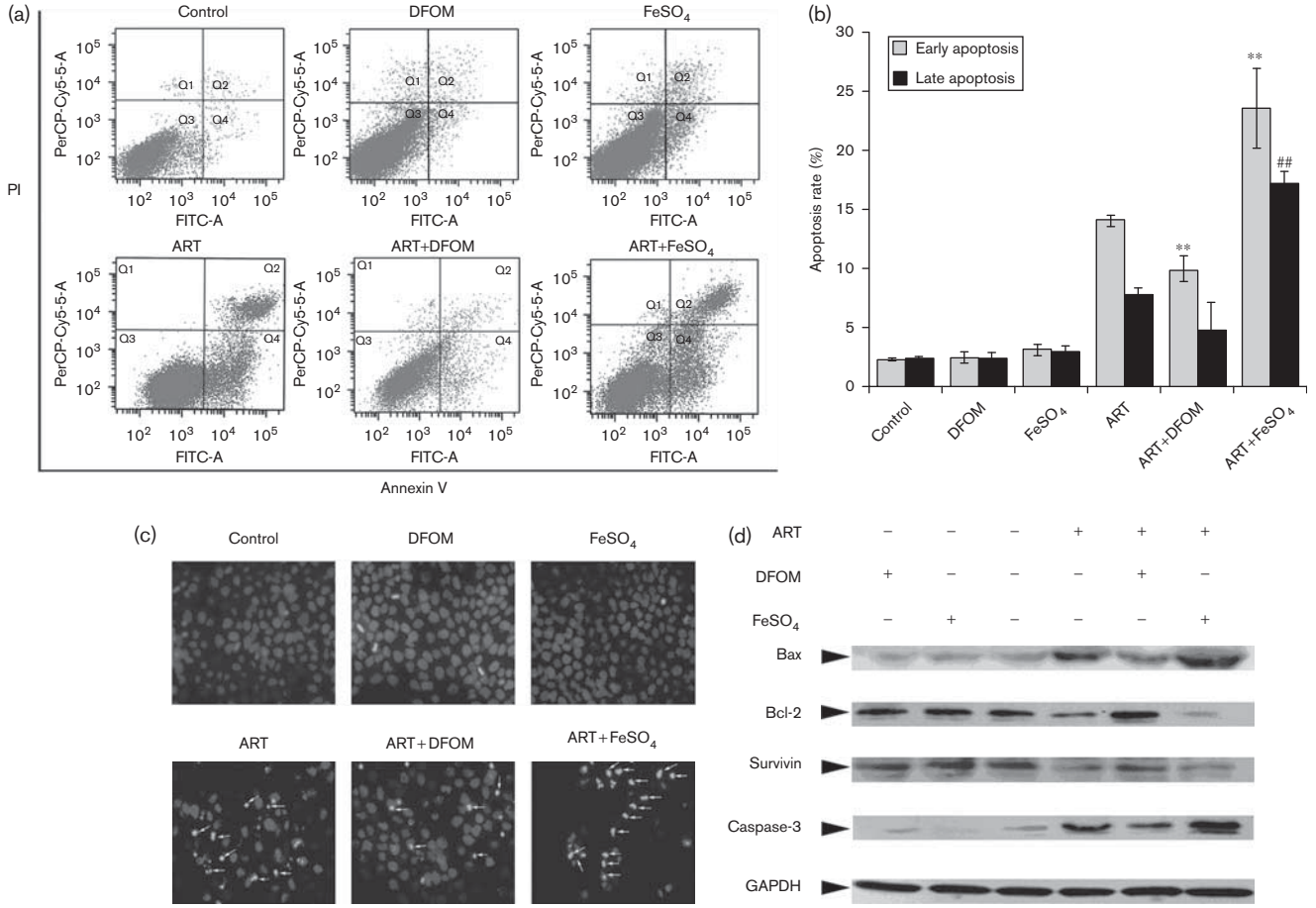

Cellular iron level is involved in artesunate (ART)-induced apoptosis. After pretreating with deferoxamine mesylate (DFOM) or $FeSO_4$ for 4 h, A431 cells were treated with 60 μmol/l ART for an additional 48 h. (a) Apoptotic cells were estimated using flow cytometric analysis after staining with annexin V/propidium iodide (PI). (b) Quantitative analysis of apoptotic cells after ART treatment. $^{**}P<0.01$, compared with the ART group of early apoptosis. $^{\#\#}P<0.01$, compared with the ART group of late apoptosis. Data shown are means ± SEM of three independent experiments. (c) To observe the apoptotic morphology, cell nuclei were visualized by DAPI staining. Arrows indicate apoptotic features (nuclear condensation and nuclear fragmentation). (d) The expression level of apoptosis-related proteins including Bax, Bcl-2, survivin, and caspase-3 were analyzed using western blots after 48 h of ART treatment with preincubation with DFOM or $FeSO_4$ for 4 h.

sensitivity and resistance of cancer cells toward ART [25,26]. We also cannot exclude the fact that other mechanisms such as angiogenesis played a role in ART-induced apoptosis, as DFOM did not completely block the apoptotic effect. Importantly, ART-induced apoptotic effects significantly intensified in cells pretreated with $FeSO_4$. Iron-overload conditions induced by $FeSO_4$ also enhanced the upregulation of Bax and caspase-3 and downregulation of Bcl-2 and survivin by ART, demonstrating its possible synergistic effect with ART. This raised the possibility of combining ART with an iron enhancer in the future treatment against skin cancer. Recently, oral coadministration of ART with ferrous sulfate (2.5 mg/kg) has been shown to significantly increase mitochondrial permeability transition pore opening in rat liver [27].

Taken together, we provided the first evidence that ART has anticancer effects in A431 human epidermoid carcinoma cells through G0/G1-phase cell cycle arrest and iron-mediated mitochondrial apoptosis. Its relatively low toxicity in normal cells and strong growth inhibitory effect in A431 cells strongly suggest that ART merits further investigation as a novel anti-skin cancer drug.

Acknowledgements

This work was supported by grants No. 30971349 and 30871310 from the National Science Foundation of China (NSFC).

Conflicts of interest

There are no conflicts of interest.

References

1 Strom SS, Yamamura Y. Epidemiology of nonmelanoma skin cancer. *Clin Plast Surg* 1997; **24**:627–636.

2 Lewis KG, Weinstock MA. Trends in nonmelanoma skin cancer mortality rates in the United States, 1969 through 2000. *J Invest Dermatol* 2007; **127**:2323–2327.

3 Klayman DL. Qinghaosu (artemisinin): an antimalarial drug from China. *Science* 1985; **228**:1049–1055.

4 Efferth T, Dunstan H, Sauerbrey A, Miyachi H, Chitambar CR. The anti-malarial artesunate is also active against cancer. *Int J Oncol* 2001; **18**:767–773.

5 Efferth T. Willmar Schwabe Award 2006: antiplasmodial and antitumor activity of artemisinin – from bench to bedside. *Planta Med* 2007; **73**:299–309.

6 Morrissey C, Gallis B, Solazzi JW, Kim BJ, Gulati R, Vakar-Lopez F, *et al.* Effect of artemisinin derivatives on apoptosis and cell cycle in prostate cancer cells. *Anticancer Drugs* 2010; **21**:423–432.

7 Hou J, Wang D, Zhang R, Wang H. Experimental therapy of hepatoma with artemisinin and its derivatives: in vitro and in vivo activity, chemosensitization, and mechanisms of action. *Clin Cancer Res* 2008; **14**:5519–5530.

8 Chen T, Li M, Zhang R, Wang H. Dihydroartemisinin induces apoptosis and sensitizes human ovarian cancer cells to carboplatin therapy. *J Cell Mol Med* 2009; **13**:1358–1370.

9 Du JH, Zhang HD, Ma ZJ, Ji KM. Artesunate induces oncosis-like cell death in vitro and has antitumor activity against pancreatic cancer xenografts in vivo. *Cancer Chemother Pharmacol* 2010; **65**:895–902.

10 Michaelis M, Kleinschmidt MC, Barth S, Rothweiler F, Geiler J, Breitling R, *et al.* Anti-cancer effects of artesunate in a panel of chemoresistant neuroblastoma cell lines. *Biochem Pharmacol* 2010; **79**:130–136.

11 Nam W, Tak J, Ryu JK, Jung M, Yook JI, Kim HJ, *et al.* Effects of artemisinin and its derivatives on growth inhibition and apoptosis of oral cancer cells. *Head Neck* 2007; **29**:335–340.

12 Efferth T, Benakis A, Romero MR, Tomicic M, Rauh R, Steinbach D, *et al.* Enhancement of cytotoxicity of artemisinins toward cancer cells by ferrous iron. *Free Radic Biol Med* 2004; **37**:998–1009.

13 Hamacher-Brady A, Stein HA, Turschner S, Toegel I, Mora R, Jennewein N, *et al.* Artesunate activates mitochondrial apoptosis in breast cancer cells via iron-catalyzed lysosomal reactive oxygen species production. *J Biol Chem* 2011; **286**:6587–6601.

14 Mercer AE, Copple IM, Maggs JL, O'Neill PM, Park BK. The role of heme and the mitochondrion in the chemical and molecular mechanisms of mammalian cell death induced by the artemisinin antimalarials. *J Biol Chem* 2011; **286**:987–996.

15 Disbrow GL, Baege AC, Kierpiec KA, Yuan H, Centeno JA, Thibodeaux CA, *et al.* Dihydroartemisinin is cytotoxic to papillomavirus-expressing epithelial cells in vitro and in vivo. *Cancer Res* 2005; **65**:10854–10861.

16 Lai H, Nakase I, Lacoste E, Singh NP, Sasaki T. Artemisinin–transferrin conjugate retards growth of breast tumors in the rat. *Anticancer Res* 2009; **29**:3807–3810.

17 Oh S, Shin WS, Ham J, Lee S. Acid-catalyzed synthesis of 10-substituted triazolyl artemisinins and their growth inhibitory activity against various cancer cells. *Bioorg Med Chem Lett* 2010; **20**:4112–4115.

18 Adams JM, Cory S. Apoptosomes: engines for caspase activation. *Curr Opin Cell Biol* 2002; **14**:715–720.

19 Schlesinger PH, Gross A, Yin XM, Yamamoto K, Saito M, Waksman G, *et al.* Comparison of the ion channel characteristics of proapoptotic BAX and antiapoptotic BCL-2. *Proc Natl Acad Sci USA* 1997; **94**:11357–11362.

20 Jiao Y, Ge CM, Meng QH, Cao JP, Tong J, Fan SJ. Dihydroartemisinin is an inhibitor of ovarian cancer cell growth. *Acta Pharmacol Sin* 2007; **28**: 1045–1056.

21 Huang XF, Yuan D, Zhang CC, Zhang XP. Artesunate induces prostate cancer cell line PC-3 differentiation and cell cycle arrest. *Zhong Xi Yi Jie He Xue Bao* 2008; **6**:591–594.

22 Cabello CM, Lamore SD, Bair WB III, Qiao S, Azimian S, Lesson JL, *et al.* The redox antimalarial dihydroartemisinin targets human metastatic melanoma cells but not primary melanocytes with induction of NOXA-dependent apoptosis. *Invest New Drugs* 2011; DOI: 10.1007/s10637-011-9676-7.

23 Zhang S, Chen H, Gerhard GS. Heme synthesis increases artemisinin-induced radical formation and cytotoxicity that can be suppressed by superoxide scavengers. *Chem Biol Interact* 2010; **186**:30–35.

24 Efferth T, Oesch F. Oxidative stress response of tumor cells: microarray-based comparison between artemisinins and anthracyclines. *Biochem Pharmacol* 2004; **68**:3–10.

25 Efferth T, Sauerbrey A, Olbrich A, Gebhart E, Rauch P, Weber HO, *et al.* Molecular modes of action of artesunate in tumor cell lines. *Mol Pharmacol* 2003; **64**:382–394.

26 Mukanganyama S, Widersten M, Naik YS, Mannervik B, Hasler JA. Inhibition of glutathione S-transferases by antimalarial drugs possible implications for circumventing anticancer drug resistance. *Int J Cancer* 2002; **97**:700–705.

27 Fafowora MV, Atanu F, Sanya O, Olorunsogo OO, Erukainure OL. Effect of oral coadministration of artesunate with ferrous sulfate on rat liver mitochondrial membrane permeability transition. *Drug Chem Toxicol* 2011; **34**:318–323.